On anticontrol of Hopf bifurcations

Diego Alonso[1], *Eduardo Paolini and Jorge Moiola*[1]

Dpto. de Ingeniería Eléctrica - Universidad Nacional del Sur
Av. Alem 1253 - (8000) Bahía Blanca - ARGENTINA
E-mail: dalonso@criba.edu.ar

Abstract

In this paper, the control of the amplitude of the oscillations in an underactuated mechanical system is treated. Two different procedures for the design of the controller are proposed. One is based on Hopf bifurcation theory, and the other is derived from considerations about the system's energy. The performance of the designed controllers is analyzed via numerical simulations. Experimental results for the energy-based law are also included.

1 Introduction

The control of oscillatory mechanical systems has received great attention for many years, arising from the one link pendulum, used as a model for numerous practical problems, to the more sophisticated underactuated mechanical systems subject to gravitational effects like Furuta's pendulum [1], the pendulum in the cart [2], the Acrobot [3], the n-link pendulum [4]. All these systems are variations of the classical pendulum leading to models of different complexities. One of the main issues, common to all of them, is the stabilization of the system around one of its unstable equilibrium points. Although there are many approaches to perform this task, one common way to reach the unstable equilibrium point is to swing the pendulum until it passes near the target point switching then to a linear stabilizing controller. This approach is still applicable when the actuators have insufficient power, and swinging is the only way to reach the unstable operating point [5]. Moreover, in many practical cases, such as those with restricted power actuators that preclude large domains of attraction for the linear controller, the way in which the pendulum approaches the target becomes crucial, and accurate control of the oscillating behavior is mandatory.

In general, these systems are non-autonomous. However, with a convenient feedback law they can be treated as autonomous ones. Then, the mathematical framework of the most common mechanism to guarantee a sustained oscillatory behavior in autonomous (smooth) nonlinear systems, the Hopf bifurcation theorem, can be applied. Under this framework, to induce such oscillatory behavior in this kind of systems, the defining conditions for a Hopf bifurcation point must be verified. Although the Hopf bifurcation mechanism is now completely understood, its control (stabilization, change of the oscillation amplitude, and so on) and its anti-control have been proposed [6-10] recently.

In this paper, the creation and stabilization of an orbit of desired amplitude in an underactuated pendulum is analyzed. Two different procedures are presented. The first one consists in introducing a Hopf bifurcation via two different state feedback laws. This procedure was presented in [11], and it is based on the Hopf bifurcation theorem. The second law is based on energy-balance arguments. It is proved that using this control law the closed loop system also undergoes a Hopf bifurcation. Both methods are compared by means of numerical simulations and verified on an experimental pendulum built in our laboratory.

2 Preliminaries

Consider the underactuated mechanical system shown in Fig. 1, consisting in a simple pendulum with an inertia disk on its free extreme. The system has two degrees of freedom: the position of the arm (θ_1) with respect to the vertical line ($\theta_1 = 0$ at the rest position), and the position of the disk (θ_2) with respect to the arm. The arm joint is not actuated, and the disk is driven by a DC motor.

The equations of motion of the system can be derived applying the Euler-Lagrange formalism. Defining the state variables $x_1 = \theta_1$, $x_2 = \dot{\theta}_1$ (angular velocity of the arm) and $x_3 = \dot{\theta}_2$ (angular velocity of the disk respect to the arm), and the control input u (voltage applied to the motor), the system's dynamic is represented by

$$\begin{aligned} \dot{x}_1 &= x_2 \\ \dot{x}_2 &= -q_1 \sin x_1 + q_2 x_3 - q_3 u \\ \dot{x}_3 &= q_1 \sin x_1 - q_2 (1+\rho) x_3 + q_3 (1+\rho) u. \end{aligned} \tag{1}$$

The parameters q_i and ρ are positive constants, related to the physical parameters of the system as follows: $q_1 = g(m_1 c + m_2 L)/I_{1eq}$, $q_2 = N^2 k_T k_F/(I_{1eq} R)$,

[1]CONICET (National Council of Scientific Research of Argentina)

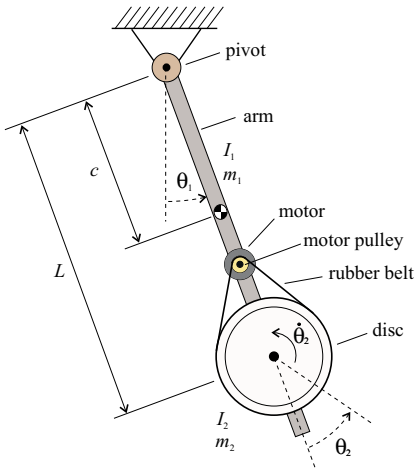

Figure 1: The underactuated pendulum.

$q_3{=}Nk_T/\left(I_{1eq}R\right)$, $\rho{=}I_{1eq}/I_2$, where $I_{1eq}{=}m_1c^2+I_1+m_2L^2$, m_1 and I_1 are the mass and the moment of inertia of the pendulum's arm, m_2 and I_2 are the mass and the moment of inertia of the disk, c is the distance from the pivot to the center of mass of the arm, L is the distance from pivot to disk's shaft, g is the gravity acceleration, N is the motor to disk reduction ratio, R is the rotor coil resistance, k_T is the torque constant and k_F is the back-emf constant. In this model the friction force of the arm bearing has been neglected.

The control objective is the stabilization of an oscillation of desired amplitude. Toward this end two different design procedures are introduced in the following.

3 Hopf bifurcation-based control law

One approach to generate oscillations on the system is to introduce a Hopf bifurcation at the equilibrium point $x_0 = (0,0,0)$ by means of an appropriate state feedback. The design procedure consists in proposing a nonlinear (smooth) feedback law such that the eigenvalues of the linearized system at x_0 can be relocated to fulfill the hypotheses of the Hopf bifurcation theorem. This procedure has been presented in [11], where two feedback laws that render the system autonomous and that do not change the equilibrium point have been developed. These control laws are briefly resumed below.

3.1 Case 1

The first control law proposed is

$$u = r_1 \sin x_1 - r_2 x_3 + k_2 x_2^3, \tag{2}$$

where r_1 is the main bifurcation parameter, $r_2{>}{-}q_2/q_3$, and $k_2{>}0$. The feedback gains r_1 and r_2 allow to varying artificially the physical parameters represented by q_1 and q_2. The term $k_2x_2^3$ is added to control the stability of the limit cycle. The defining conditions of a Hopf bifurcation occurs for $r_1^c{=}{-}q_1/\left(q_3\left(1+\rho\right)\right)$, and the stability of the emerging limit cycle is ensured by the negativity of the first curvature index (also called first Lyapunov coefficient or curvature coefficient)

$$\sigma_{1_{\rm I}} = -\frac{3}{8}\frac{\rho^2 k_2 q_1^2 q_3}{\left(1+\rho+\rho q_1\right)(\rho q_1+(1+\rho)^3(q_2+q_3r_2)^2)}.$$

This index has been computed using the formula in the so-called frequency domain approach [12].

3.2 Case 2

The second feedback law is

$$u = k_1 x_2 + k_2 x_2^3, \tag{3}$$

where k_1 is the main bifurcation parameter and $k_2 > 0$. This law modifies the linearized system by adding the term k_1x_2. Again, the term $k_2x_2^3$ is added to control the stability of the emerging limit cycle. The critical value of k_1 is $k_1^c = -q_2/q_3$, and the stability of the emerging cycle is verified by computing the first curvature index

$$\sigma_{1_{\rm II}} = -\frac{3}{8}\frac{k_2 q_1^2 q_3}{\left(1+q_1\right)(\rho^2 q_2^2+q_1)}.$$

On both cases, to obtain an oscillation of desired amplitude, appropriate values for the controller parameters can be chosen computing the continuation of the periodic solutions in terms of the main bifurcation parameter (r_1 in the first case, and k_1 in the second one). In addition, by means of the frequency domain approach it is possible to approximate the amplitude and the frequency of the limit cycle for given values of the controller's parameters.

4 Energy-based control law

In this Section, a control law based on energetic concepts is derived. The design procedure is based on physical considerations as in [5], instead of a rigorous proof based, for example, on Lyapunov theory.

The energy of the system (except for a normalization factor) is given by

$$H = \frac{1}{2}\rho x_2^2 + \rho q_1\left(1-\cos\left(x_1\right)\right) + \frac{1}{2}\left(x_2+x_3\right)^2,$$

which can be decomposed as the sum of an energy term associated to the arm of the pendulum (considering the disk as a point-mass)

$$H_a = \frac{1}{2}\rho x_2^2 + \rho q_1\left(1-\cos\left(x_1\right)\right),$$

and a term associated to the kinetic energy of the disk

$$H_d = \frac{1}{2}x_d^2,$$

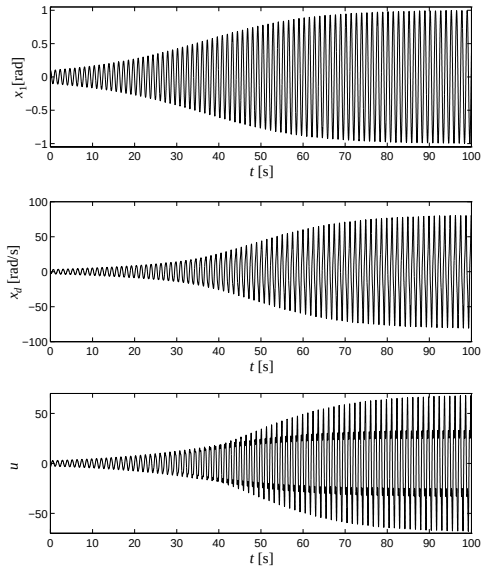

Figure 2: Simulation results obtained with the first Hopf-based controller (r_1=−40, $r_2 = 0.5$, $k_2 = 0.75$).

where $x_d = x_2 + x_3$ is the velocity of the inertia disk respect to a reference frame fixed to the lab.

Let $x_{1\,\max}$ be the desired amplitude of oscillation, which corresponds to the energy level of the arm

$$H^* = \rho q_1 \left(1 - \cos\left(x_{1\,\max}\right)\right).$$

The control objective is that the energy associated to the arm reaches the desired level ($H_a \to H^*$) and the energy associated to the disk goes to zero ($H_d \to 0$).

Since the disk position is the only actuated variable, injecting or absorbing energy from the system can be done only by varying the way in which the energy is supplied to the disk, *i.e.* by varying the disk velocity in such a way that an energy transference from the disk to the arm do occur. To reach a certain energy level H^*, it is proposed to change the kinetic energy of the disk in a quantity equal to $\Delta H = H^* - H_a$. Thus we set $H_d = 1/2\ x_d^2 = |\Delta H|$, from which the disk velocity corresponding to this energy level can by computed

$$x_d = \pm\sqrt{2\,|\Delta H|}. \tag{4}$$

The sign of the (desired) disk velocity defines two different behaviors of the system. In one case, due to the mechanical coupling between the disk and the arm, the desired energy level H^* will be captured solely by the disk, with the arm (ideally) at the rest position. The second case corresponds to the arm swinging at the energy level H^*, interchanging kinetic energy (T_a) and potential energy (V_a), such that $H^* = T_a + V_a$, and the disk remains with zero velocity respect to a reference frame fixed at the lab. In this case the disk acts as

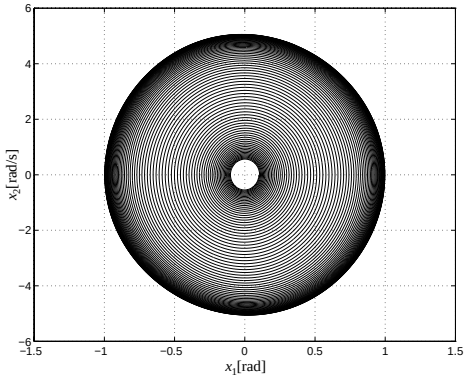

Figure 3: Limit cycle obtained with the first Hopf-based controller ($r_1 = -40$, $r_2 = 0.5$, $k_2 = 0.75$).

a point-mass, and no inertial effects can be observed because the disk velocity is zero.

The transference of energy between the disk and the arm occurs when the disk speed is varied, since this acceleration ($\dot{x}_d$) produces a torque on the bar. In order to increase or decrease the amplitude of the pendulum swinging, this torque should be applied in the proper sense. To determine the correct sign of the disk acceleration (and velocity) it is convenient to compute the temporal derivatives of H_a

$$\begin{aligned} \dot{H}_a &= \rho x_2 \dot{x}_2 + \rho q_1 \sin\left(x_1\right)\dot{x}_1 \\ &= \rho x_2 \left(q_2 x_3 - q_3 u\right) \\ &= -x_2 \dot{x}_d, \end{aligned} \tag{5}$$

From (5) it is clear that H_a is incremented if $\mathrm{sgn}(\dot{x}_d) = -\mathrm{sgn}(x_2)$, and decremented if $\mathrm{sgn}(\dot{x}_d) = \mathrm{sgn}(x_2)$. Then, the correct sign of $\dot{x}_d$ is

$$\mathrm{sgn}\left(\dot{x}_d\right) = -\mathrm{sgn}\left(x_2\right)\mathrm{sgn}\left(\Delta H\right). \tag{6}$$

To verify (6), from (4) we choose

$$x_d = -\mathrm{sgn}\left(x_2 \Delta H\right)\sqrt{2\,|\Delta H|}, \tag{7}$$

or, its equivalent $x_3 = -x_2 - \mathrm{sgn}(x_2 \Delta H)\sqrt{2\,|\Delta H|}$.

Since the disk velocity can not be immediately established, due to the disk's inertia, a kind of proportional control for x_3 is proposed

$$u = \frac{k}{q_3}\left(x_{3r} - x_3\right) + \frac{q_2}{q_3} x_3, \tag{8}$$

with

$$x_{3r} = -x_2 - \mathrm{sgn}\left(x_2 \Delta H\right)\sqrt{2\,|\Delta H|}. \tag{9}$$

Note that x_{3r} is the "desired" velocity of the disk. Then, the closed loop version of system (1) with (8)-(9) is

$$\begin{aligned} \dot{x}_1 &= x_2 \\ \dot{x}_2 &= -q_1 \sin x_1 + k x_3 - k x_{3r} \\ \dot{x}_3 &= q_1 \sin x_1 - k\left(1+\rho\right) x_3 + k\left(1+\rho\right) x_{3r}, \end{aligned} \tag{10}$$

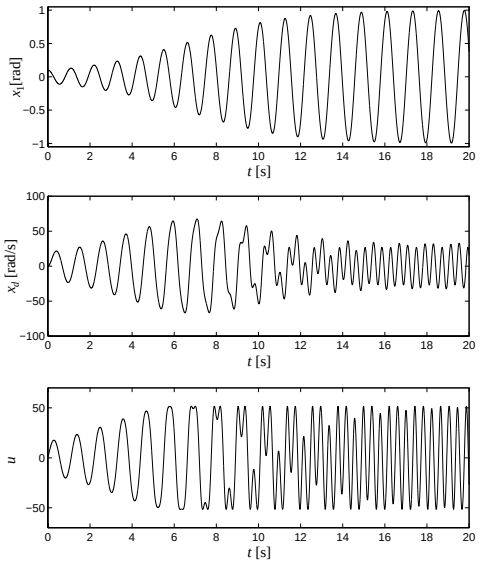

Figure 4: Simulation results obtained with the second Hopf-based controller ($k_1 = -30$, $k_2 = 1.5$).

that can also be written as

$$\begin{aligned} \dot{x}_1 &= x_2 \\ \dot{x}_2 &= -q_1 \sin x_1 + k x_d - k x_{dr} \\ \dot{x}_d &= -k\rho x_d + k\rho x_{dr}, \end{aligned} \tag{11}$$

where $x_{dr} = -\mathrm{sgn}(x_2 \Delta H)\sqrt{2\,|\Delta H|}$. This form reveals some interesting properties. The last equation of (11) express the acceleration of the disk, and it can be seen that the disk speed is a low-pass filtered version of x_{dr},

$$\dot{x}_d = -k\rho x_d + k\rho x_{dr}, \tag{12}$$

with time constant $1/(k\rho)$ and unity gain.

To ensure that the target orbit is reached, x_d must verify (7), but since x_d is a filtered version of x_{dr}, the phase-shift introduced by the filter can lead to the failure of this condition. Although a rigorous verification of the asymptotic behavior and stability of the orbit is cumbersome, due to the presence of the square root and sign functions in the control law, the approximate analysis of the next subsection shows that the system behaves following the classical Hopf bifurcation theorem. In addition, both numerical simulations and experimental results confirm that the orbit is reached.

Finally, note that for $H_a \to H^*$, $x_{dr} \to 0$, and thus from (12), $x_d \to 0$, or equivalently $x_3 \to -x_2$. Hence, the closed loop system behaves like a simple pendulum with a natural frequency of oscillation $\omega = \sqrt{q_1}$.

4.1 Hopf analysis

In this subsection we prove that the closed loop system undergoes a Hopf bifurcation for H^*=0 by using the

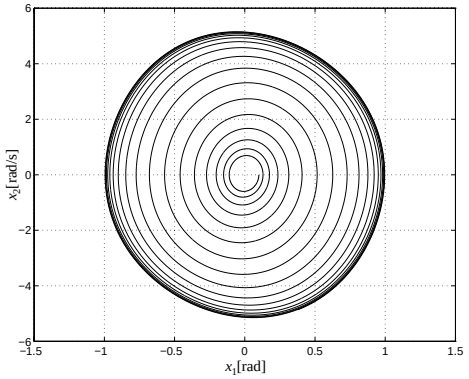

Figure 5: Limit cycle obtained with the second Hopf-based controller ($k_1 = -30$, $k_2 = 1.5$).

control law (8). To apply the Hopf bifurcation theory it is necessary to make some approximations to the control law, to avoid the discontinuity introduced by the sign function. Toward this end let us consider u as in (8) but with

$$x_{3r} = -x_2 - \tanh(c x_2 \Delta H)\sqrt{2\tanh(c\Delta H)\,\Delta H}, \tag{13}$$

where c>0 is a constant arbitrarily large. From a practical point of view, this is a reasonable approximation.

The closed loop linearization matrix at the origin is

$$A = \begin{bmatrix} 0 & 1 & 0 \\ -q_1 & k\,l\,(H^*) & k \\ q_1 & -k\,(1+\rho)\;\; l\,(H^*) & -k\,(1+\rho) \end{bmatrix},$$

where $l\,(H^*) \triangleq 1 + cH^*\sqrt{2\tanh(cH^*)\,H^*}$. To satisfy the defining conditions of a Hopf bifurcation, matrix A should have a pair of complex conjugate eigenvalues crossing the imaginary axis from the left to the right half-plane, and the real eigenvalue must remain negative. Since H^* is an energy level, it has no sense to consider negative values of H^*. For the critical value $H_c^* = 0$, the linearized system has a pair of complex conjugate eigenvalues at $\lambda_{1,2} = \pm\sqrt{q_1}$, and a real one at $\lambda_3 = -k\rho$. By incrementing H^* the complex eigenvalues moves to the right half plane. The stability of the emerging limit cycle is analyzed by computing the first curvature index at the critical frequency $\omega_c = \sqrt{q_1}$, which is given by

$$\sigma_1 = -\frac{kcq_1^2\left(3\rho+2\rho cH^*\sinh^{-1}(2cH^*)+c^2H^{*3}\right)\sqrt{H^*\tanh(cH^*)}}{4\sqrt{2}(k^2\rho^2+q_1)(1+q_1)\;l(H^*)},$$

and taking the limit for $H^* \to 0$ results in

$$\sigma_{1c} = \lim_{H^*\to 0}\sigma_1 = 0.$$

Notice that it is not possible to distinguish if the focus is a vague attractor (emergence of a stable limit cycle when the parameter moves from the criticallity) or a

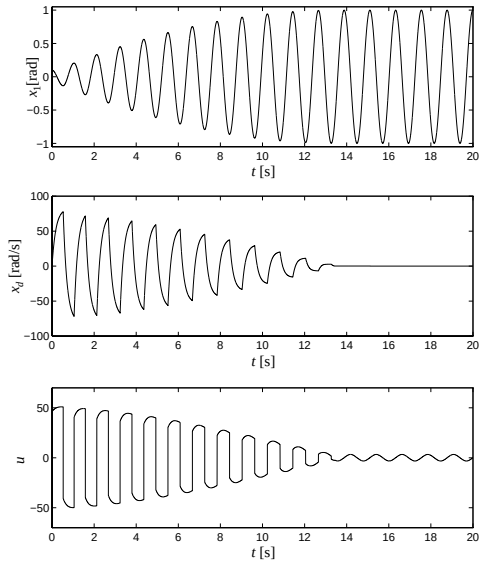

Figure 6: Simulation results obtained with the energy-based controller ($H^* = 3447.7, k = k^*$=0.0219).

vague repeller (starting an unstable limit cycle) since the curvature coefficient does not have sign definition at criticallity. Nevertheless, once H^* takes positive values, σ_1 is negative for $k > 0$ and $c > 0$. Moreover, when $H^* \to 0$ this energy level corresponds to the rest position and the swinging should extinguish itself. To prove this, a computation of the second Lyapunov coefficient should be carried out. In this paper, we do not treat this degenerate case since we are interested in $H^* > 0$, in order to guarantee a true oscillation of the system.

4.2 Considerations about parameter k

Note that for $H^* > 0$ (but near H_c^*), and $c > 0$, σ_1 has a minimum for $k^* = \sqrt{q_1}/\rho$. This value of k is connected to the optimum rate of convergence to the desired orbit, in the sense that the system reaches the desired orbit in minimum time when $k = k^*$. A physical interpretation helps to understand this fact. Rearranging (5)

$$\dot{H}_a = k\rho x_2 \left(x_d - x_{dr}\right).$$

This means that the rate of change of the arm energy depends on the signal $x_d - x_{dr}$, which is a high-pass filtered version of x_{dr} with time constant $k\rho$ [see (11)]. The fundametal frequency of x_{dr} is that of x_2, and since the natural frequency of the pendulum near the origin is $\omega = \sqrt{q_1}$, then the fundamental frequency of x_{dr} is approximately $\sqrt{q_1}$. Therefore, k can be chosen to maximize the modulus of the filtered signal at $\omega = \sqrt{q_1}$, resulting in $k = k^*$.

4.3 Robustness with respect to q_2 and q_3

Suppose that in (8) we use parameters $\tilde{q}_2$ and $\tilde{q}_3$ instead of the true parameters q_2 and q_3. It can be shown that

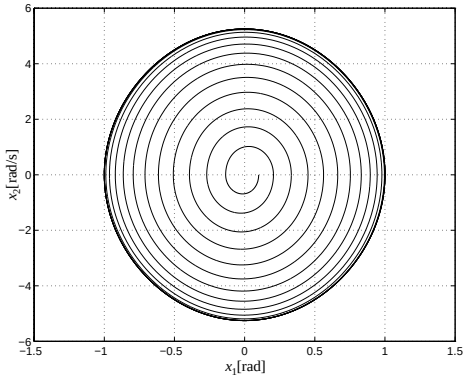

Figure 7: Limit cycle obtained with the energy-based controller ($H^* = 3447.7$, $k = k^* = 0.0219$).

the existence of a stable Hopf bifurcation is assured for

$$k > \tilde{q}_3 \left(\frac{\tilde{q}_2}{\tilde{q}_3} - \frac{q_2}{q_3}\right). \tag{14}$$

Moreover, by defining the relative error $e_i \triangleq (\tilde{q}_i - q_i)/q_i$ for i=2, 3, the stability condition (14) results in

$$k > q_2 \left(e_2 - e_3\right). \tag{15}$$

From (15), if $e_3 > e_2$ the controller is robust for any k>0.

5 Simulations and experimental results

All the three designed controllers were tested via numerical simulations for the system parameters $q_1 = 30$ s^{-2}, $q_2 = 0.0245$ s^{-1}, $q_3 = 0.0393$ s^{-1} and $\rho = 250$, to compare the design procedures.

For an amplitude of oscillation of 1 rad, the parameters of the controllers were chosen such that the maximum amplitude of the control actions are similar and do not exceed 60 units (1 unit of $u \cong 0.18$ V). In Fig. 2, the response of the system with the controller given by (2), with parameters $r_1 = -40$, $r_2 = 0.5$, and $k_2 = 0.75$, is shown. Figure 3 shows the oscillation in the phase plane $x_1 - x_2$. The response of the system with the controller given by (3), with parameters $k_1 = -30$, and $k_2 = 1.5$, is shown in Fig. 4. Figure 5 shows the oscillation in the phase plane $x_1 - x_2$. A comparison of these two controllers, reveals that the time spent by the system to reach the desired amplitude is considerably greater in the first case for comparable control efforts. This fact, together with the simplicity of the controller, makes the second one a better design compared to the first one.

The performance of the system under the energy-based controller is shown in Figs. 6 and 7, for $H^* = \rho q_1 \left(1 - \cos\left(1\right)\right) = 3447.7$ and $k = \sqrt{q_1}/\rho = 0.0219$. In this case, it seems that the control action is applied in a better way, since the system reaches the desired amplitude in less time. Moreover, since x_d tends to zero

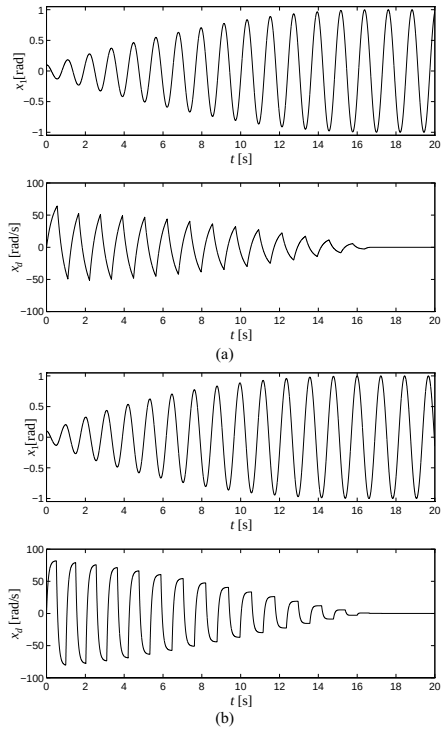

Figure 8: Simulation results obtained with the energy-based controller. (a) $H^* = 3447.7, k = 0.011 \simeq k^*/2$, (b) $H^* = 3447.7, k = 0.044 \simeq 2k^*$.

the control action takes the necessary value to make $x_3 = -x_2$, which is significantly less than any of the controllers of the cases 1 and 2. Furthermore, the "optimum" value of k ($k^* = \sqrt{q_1}/\rho$) is corroborated by simulations. In Fig. 8a and 8b, the behavior of the closed loop system with $k \simeq k^*/2$ and $k \simeq 2k^*$, respectively, are shown. Note that in both cases the system reaches the target orbit in a larger time than using $k = k^*$.

Finally, this controller has been implemented on an actual pendulum and the resulting behavior can be seen in Fig. 9, which agrees with the simulation. For the Hopf based control laws, experimental results also agree with numerical ones, and they have been reported in [11].

6 Conclusions

The problem of amplitude control in an oscillatory mechanical system has been discussed. Two different procedures to design the controller has been presented. The first one is based on the Hopf bifurcation theory, which has a purely mathematical flavor. The second arises from the analysis of the system's energy, and takes advantages from physical properties of the system. The performance of the designed controllers have been compared by means of simulations. These comparisons show a better behavior of the feedback system with the energy-based controller. Finally, the experimental results for the last design have been included, which show a good agreement with the simulations.

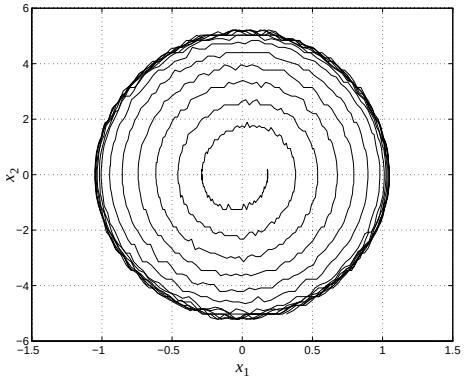

Figure 9: Limit cycle experimentally obtained with the energy-based controller (H^*=3447.7, k=0.05).

References

[1] K. Furuta, M. Yamakita, and S. Kobayashi, "Swing-up control of inverted pendulum using pseudo-state feedback," *Proc.Instn.Mech.Engrs.*, 206, pp. 263-269, 1992.

[2] Q. Wei, W. P. Dayawansa, and W. S. Levine, "Nonlinear controller for an inverted pendulum having restricted travel," *Automatica*, vol. 31, no. 6, pp. 841-850, 1995.

[3] M. W. Spong, "The swing up control problem for the acrobot," *IEEE Contr. Syst. Mag.*, vol. 20, pp. 49-55, 1995.

[4] S. P. Weibel, and J. Baillieul, "Open-loop oscillatory stabilization of an n-pendulum," *Int. J. Contr.*, vol. 71, no. 5, pp. 931-957, 1998.

[5] K. J. Aström, and K. Furuta, "Swinging up a pendulum by energy control," *Proc. 13th IFAC World Congress*, San Francisco, 1996, pp. 37-42.

[6] E. H. Abed, and J. H. Fu, "Local feedback stabilization and bifurcation control, Part I. Hopf bifurcation," *Sys. Contr. Lett.*, vol. 7, pp. 11-17, 1986.

[7] J. L. Moiola, D. W. Berns, and G. Chen, "Feedback control of limit cycle amplitudes," *Proc. 36th IEEE Conf. Decision Contr.*, San Diego, CA, 1997, pp. 1479-1485.

[8] D. Chen, H. O. Wang, L. E. Howle, M. R. Gustafson, and T. Meressi, "Amplitude control of bifurcations and application to Rayleigh-Bénard convection," *Proc. 37th IEEE Conf. Decision Contr.*, Tampa, FL, 1998, pp. 1951-1956.

[9] Y. Wang, and R. M. Murray, "Feedback stabilization of steady-state and Hopf bifurcations," *Proc. 37th IEEE Conf. Decision Contr.*, Tampa, FL, 1998, pp. 2431-2437.

[10] D. Chen, H. O. Wang, and G. Chen, "Anti-control of Hopf bifurcations through washout filters," *Proc. 37th IEEE Conf. Decision Contr.*, Tampa, FL, 1998, pp. 3040-3045.

[11] D. Alonso, E. Paolini, and J. L. Moiola, "Bifurcation control in an underactuated pendulum," *Proc. Int. Symp. Circ. Syst.*, Geneva, Switzerland, 2000, vol. II, pp. 385-388.

[12] A. I. Mees, *Dynamics of Feedback Systems*, John Wiley & Sons, Chichester, UK, 1981.